TransNetR: Transformer-based Residual Network for Polyp Segmentation with Multi-Center Out-of-Distribution Testing

Anonymous submission[1] ANONYMOUS
[1] *Anonymous*

Editors: Under Review for MIDL 2023

Abstract

Colonoscopy is considered the most effective screening test to detect colorectal cancer (CRC) and its precursor lesions, i.e., polyps. However, the procedure experiences high miss rates due to polyp heterogeneity and inter-observer dependency. Hence, several deep learning powered systems have been proposed considering the criticality of polyp detection and segmentation in clinical practices. Despite achieving improved outcomes, the existing automated approaches are inefficient in attaining real-time processing speed. Moreover, they suffer from a significant performance drop when evaluated on inter-patient data, especially those collected from different centers. Therefore, we intend to develop a novel real-time deep learning based architecture, Transformer based Residual network (TransNetR), for colon polyp segmentation and evaluate its diagnostic performance. The proposed architecture, TransNetR, is an encoder-decoder network that consists of a pre-trained ResNet50 as the encoder, three decoder blocks, and an upsampling layer at the end of the network. TransNetR obtains a high dice coefficient of 0.8706 and a mean Intersection over union of 0.8016 and retains a real-time processing speed of 54.60 on the Kvasir-SEG dataset. Apart from this, the major contribution of the work lies in exploring the generalizability of the TransNetR by testing the proposed algorithm on the out-of-distribution (test distribution is unknown and different from training distribution) dataset. As a use case, we tested our proposed algorithm on the PolypGen (6 unique centers) dataset and two other popular polyp segmentation benchmarking datasets. We obtained state-of-the-art performance on all three datasets during out-of-distribution testing. The source code of TransNetR will be made publicly available at https://github.com/Anonymous/TransNetR.

Keywords: Out-of-distribution generalization, Out-of-distribution testing, Transformer, Polyp segmentation, Residual network, PolypGen

1. Introduction

Colorectal cancer (CRC) is the third most prevalent malignancy and accounts for 9.4% of cancer-related deaths worldwide (Sung et al., 2021). The alarmingly increasing cases of CRC have led to the adoption of various screening tests (Kanth and Inadomi, 2021) to lower the risk of its incidence and related mortalities. The colonoscopy procedure is the most preferred among these tests, which allows clinicians to identify and examine CRC precursor lesions, i.e., polyps. The early detection and resection of such polyps are crucial to prevent them from developing into cancer at their later stages. An efficient removal process of polyps requires that the clinicians have access to their accurate location information and precise boundary details. Thus, in clinical settings, polyp segmentation is a crucial task.

© 2023 A. submission.

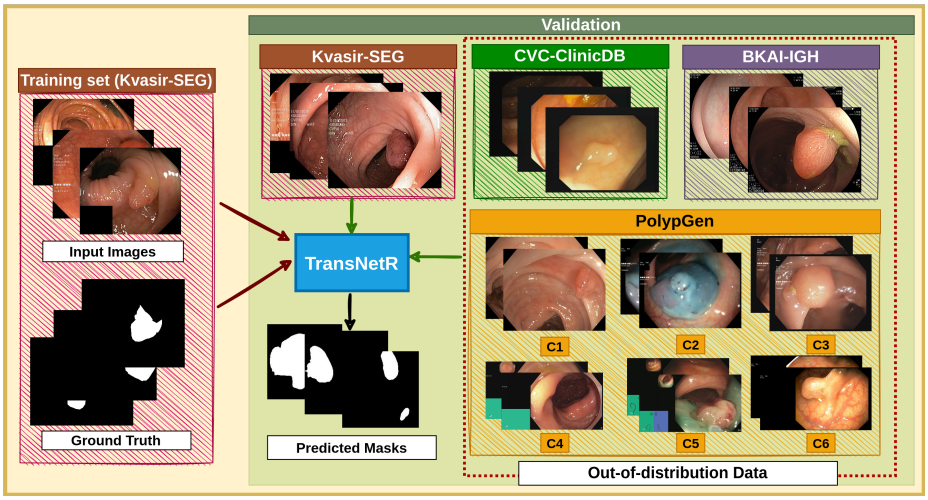

Figure 1: Illustration of different scenarios expected to arise in real-world settings. The proposed work conducted both in-distribution and out-of-distribution validation process. C1 to C6 represent the different centers data present in PolypGen (Ali et al., 2023) dataset.

Despite the wide acceptance of colonoscopy as the gold standard for CRC screening, the associated traditional assessment procedures experience significant polyp miss rates attributed to various factors (Kim et al., 2017). First, the process involves dependency on the operator's experience and the risk of overlooking polyps due to faster colonoscope withdrawal time. Second, high variations in polyps' appearance, such as color, size, and shape, further complicate the detection task. Third, the lack of intense contrast between fuzzy polyp boundaries and surrounding mucosa makes polyps camouflaged (Fan et al., 2021) against other endoluminal structures. These challenging factors present a need for automated systems to perform polyp segmentation, which could complement surgeons' ability to detect and delineate polyp boundaries for accurate resection.

In this context, many deep learning (DL) based techniques (Akbari et al., 2018; Duc et al., 2022) have been developed in the past few years. Although these methods have reported considerable improvements over manual assessments and hand-crafted features based approaches (Bernal et al., 2015; Tajbakhsh et al., 2015), they still lack generalizability. As a result, the automated techniques proposed so far are considerably prone to limited performance under real-world scenarios where they are expected to be utilized for different patients, hospitals with varying imaging modalities, or even across varied populations. Such cases involve significant variations in colon polyps due to demographic changes, including gender, age, race, and region (Yang et al., 2020). For example, a study (Cekodhima et al., 2016) observed polyp morphology and its malignant potential to be related to a patient's age. Similar disparities are reported based on geographical distribution, where the prevalence and location of large polyps are affected by race and ethnicity (Lieberman et al., 2014).

Apart from population variations, the differences in colonoscopy conducting centers and their associated video-capturing modality types also create domain shift problems (Chen et al., 2021). Some sample images collected from different datasets and multiple centers are shown in Fig. 1. The figure illustrates different validation scenarios and also demonstrates the range of heterogeneity possessed by polyps. Although the segmentation performance

achieved by SOTA methods is noteworthy, the issue of generalizability remains marginally explored as compared to testing the performance on in-distribution (iD) polyp data. One of the reasons might be the lack of availability of multi-center datasets. In this work, we propose a DL model, which is a transformer based residual network (TransNetR), to achieve accurate and real-time polyp segmentation and to generalize well on unseen out-of-distribution (OOD) data. Our architecture is inspired by the remarkable success of encoder-decoder structures, Transformers and residual learning in biomedical image analysis. To validate the efficacy of our algorithm, we test the algorithm on different datasets, which are collected from various parts of the world and unique from our training samples. The main contributions of our work are summarized below:

- We present a novel DL based polyp segmentation model. The architecture integrates the strength of transformer and residual learning to generate precise segmentation outcomes even while testing on OOD data and maintains high performance along with real-time processing speed, which is important for clinical intergration.
- The proposed architecture is extensively validated on iD and OOD datasets. The obtained results from three datasets (8 unique centers) signifies that the model performs consistently well on datasets from unseen clinical centers, showing a better generalization ability as compared to the other SOTA approach.

2. Method

In this section, we will present the proposed architecture in detail along with its components.

2.1. TransNetR

Figure 2 shows the block diagram of the proposed TransNetR. As observed in the Figure, TransNetR is an encoder decoder network which begins with a pre-trained ResNet50 as the encoder. We pass input image to the pre-trained encoder and extract four different intermediate feature maps from it. These intermediate feature maps are then passed through a 1×1 convolution layer, which is followed by a batch normalization and a LeakyReLU activation function. The 1×1 convolution layer helps in reducing the number of output feature channels which reduces the number of parameters. Next follows the decoder network, which contains three decoder blocks. The reduced feature map is fed to the first decoder block, where it is first passed through a bilinear upsampling layer. The upsampling layer increases the spatial dimensions of the feature maps by a factor of two. The upsampled feature map is then concatenated with the next reduced feature map having the same spatial dimensions.

The concatenation creates a shortcut connection from the pre-trained encoder to the decoder block, which helps in a better flow of information from encoder to decoder. The short connection fetches the feature maps, which might be lost due to the depth of the network. The concatenated feature maps are further passed through our proposed Residual Transformer block, where the feature maps are first reshaped into patches and then passed to the transformer layers. These layers consist of the multi-head self-attention, which helps in learning better feature representation. Subsequently, the output from the first decoder block is passed to the second and then to the final decoder block. In the final decoder

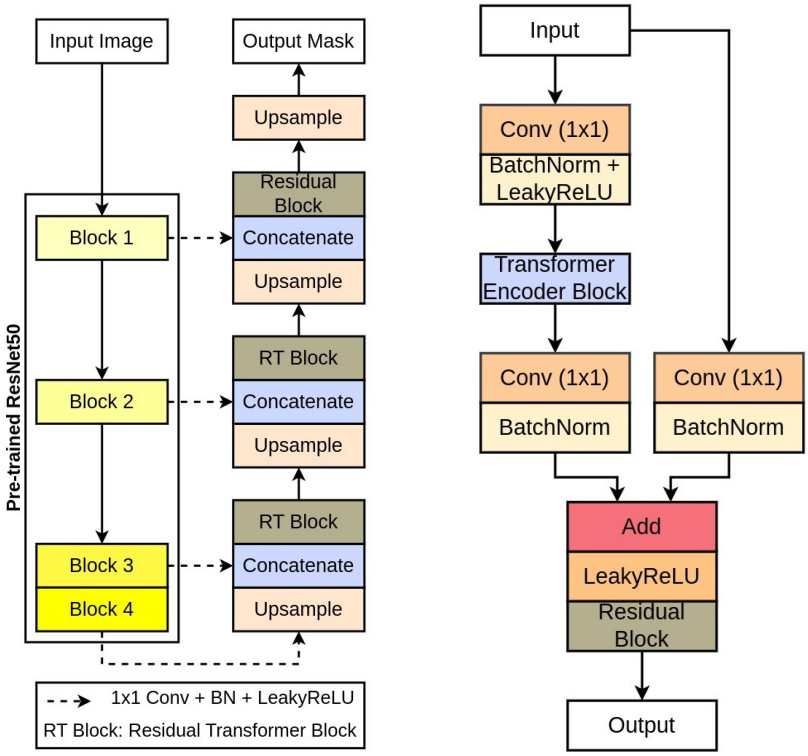

(a) Block diagram of proposed TranNetR

(b) Residual Transformer Block

Figure 2: Block diagram of TransNetR along with the Residual Transformer block

block, the Residual Transformer block is replaced with a simple residual block to reduce the number of trainable parameters. The output from the final decoder is passed through a bilinear upsampling layer which increases the spatial dimensions of the feature maps by a factor of two. The upsampled feature map is then passed through a 1×1 convolution layer with a sigmoid activation function.

2.2. Residual Transformer Block

The residual transformer block begins with a 1×1 convolution layer, followed by a batch normalization and a LeakyReLU activation function. After that, we flattened the feature maps, where we use a constant patch size of four. The flattened feature maps are then passed to the transformer block, having four heads and two layers. The transformer block provides self-attention on the feature maps, which makes the network more robust. The output from the transformer block is then reshaped back in the same shape as the input. Next, the feature map is passed through a 1×1 convolution, followed by batch normalization. After that, it is followed by addition with the input feature maps and then passed through the LeakyReLU activation function. Finally, the output from the LeakyReLU is passed through a residual block which acts as the output of the residual transformer block.

Table 1: Quantitative results on the Kvasir-SEG test dataset.

Method	mIoU	DSC	Rec.	Prec.	F2	FPS	Para.	Flops
U-Net (Ronneberger et al., 2015)	0.7472	0.8264	0.8504	0.8703	0.8353	**106.88**	31.04	54.75
U-Net++ (Zhou et al., 2018)	0.7420	0.8228	0.8437	0.8607	0.8295	81.34	9.16	34.65
ResU-Net++ (Jha et al., 2019)	0.5341	0.6453	0.6964	0.7080	0.6576	43.11	4.06	15.81
HarDNet-MSEG (Huang et al., 2021)	0.7459	0.8260	0.8485	0.8652	0.8358	34.80	33.34	6.02
ColonSegNet (Jha et al., 2021)	0.6980	0.7920	0.8193	0.8432	0.7999	73.95	5.01	62.16
UACANet (Kim et al., 2021)	0.7692	0.8502	0.8799	0.8706	0.8626	25.85	69.16	31.51
UNeXt (Valanarasu and Patel, 2022)	0.6284	0.7318	0.7840	0.7656	0.7507	87.47	**1.47**	**0.57**
TransNetR (Ours)	**0.8016**	**0.8706**	**0.8843**	**0.9073**	**0.8744**	54.60	27.27	10.58

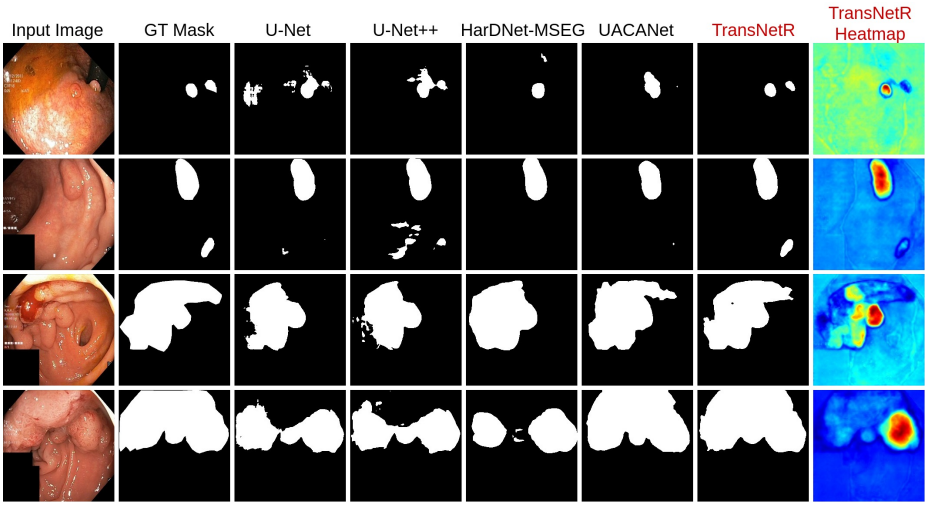

Figure 3: Qualitative example showing polyp segmentation on Kvasir-SEG (Jha et al., 2020)

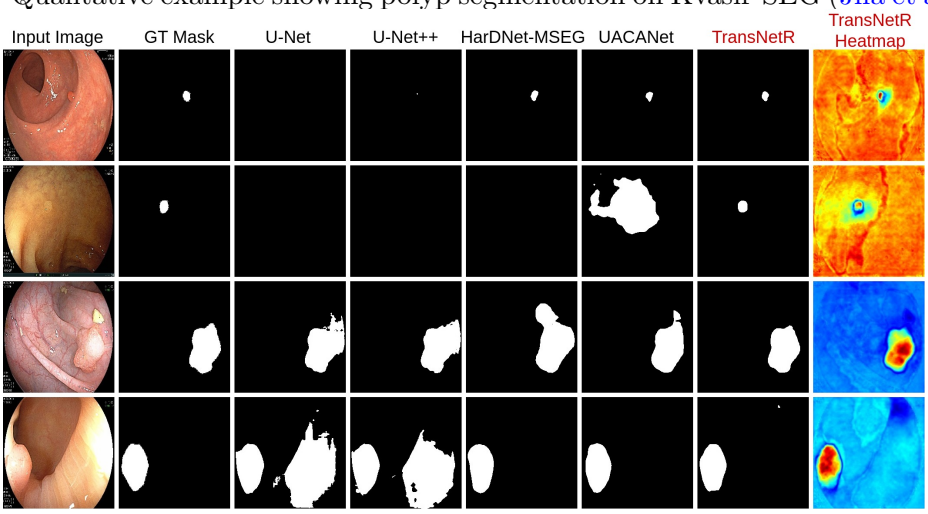

Figure 4: Cross-data result when models trained on Kvasir-SEG & tested on BKAI-IGH.

3. Experiments and Results

3.1. Dataset details and Experiment setup

We evaluate our model's performance using four datasets; namely, Kvasir-SEG (Jha et al., 2020), PolypGen (Ali et al., 2023), CVC-ClinicDB (Bernal et al., 2015), and BKAI-IGH (Ngoc Lan

Table 2: Results of the models when trained on Kvasir-SEG and tested on OOD dataset.

Method	mIoU	mDSC	Recall	Precision	F2
Training dataset: Kvasir-SEG – Test dataset: CVC-ClinicDB					
U-Net (Ronneberger et al., 2015)	0.5433	0.6336	0.6982	0.7891	0.6563
U-Net++ (Zhou et al., 2018)	0.5475	0.6350	0.6933	0.7967	0.6556
ResU-Net++ (Jha et al., 2019)	0.3585	0.4642	0.5880	0.5770	0.5084
HarDNet-MSEG (Huang et al., 2021)	0.6058	0.6960	0.7173	0.8528	0.7010
ColonSegNet (Jha et al., 2021)	0.5090	0.6126	0.6564	0.7521	0.6246
UACANet (Kim et al., 2021)	0.6808	**0.7659**	**0.7639**	0.8820	**0.7599**
UNeXt (Valanarasu and Patel, 2022)	0.3901	0.4915	0.6125	0.6609	0.5318
TransNetR (Ours)	**0.6912**	0.7655	0.7571	**0.9200**	0.7565
Training dataset: Kvasir-SEG – Test dataset: BKAI-IGH					
U-Net (Ronneberger et al., 2015)	0.5686	0.6347	0.6986	0.7882	0.6591
U-Net++ (Zhou et al., 2018)	0.5592	0.6269	0.6900	0.7968	0.6493
ResU-Net++ (Jha et al., 2019)	0.3204	0.4166	0.6979	0.3922	0.5019
HarDNet-MSEG (Huang et al., 2021)	0.5711	0.6502	**0.7420**	0.7469	**0.6830**
ColonSegNet (Jha et al., 2021)	0.4910	0.5765	0.7191	0.6644	0.6225
UACANet (Kim et al., 2021)	0.5734	0.6531	0.7361	0.7689	0.6790
UNeXt (Valanarasu and Patel, 2022)	0.3304	0.4156	0.6085	0.4933	0.4722
TransNetR (Ours)	**0.5998**	**0.6601**	0.6660	**0.9072**	0.6584

Table 3: Results of models trained on Kvasir-SEG & tested on PolypGen 23 video sequences.

Method	mIoU	mDSC	Recall	Precision	F2
Training dataset: Kvasir-SEG – Test dataset: PolypGen Video Sequence					
U-Net (Ronneberger et al., 2015)	0.4049	0.4559	0.6307	0.5762	0.4668
U-Net++ (Zhou et al., 2018)	0.4272	0.4772	0.6198	0.6269	0.4876
ResU-Net++ (Jha et al., 2019)	0.1589	0.2105	0.5095	0.2447	0.2303
HarDNet-MSEG (Huang et al., 2021)	0.4171	0.4662	0.6217	0.6120	0.4757
ColonSegNet (Jha et al., 2021)	0.3058	0.3574	0.5296	0.4804	0.3533
UACANet (Kim et al., 2021)	0.4155	0.4748	**0.6357**	0.6108	0.4886
UNeXt (Valanarasu and Patel, 2022)	0.2457	0.2998	0.5658	0.3661	0.3201
TransNetR (Ours)	**0.4717**	**0.5168**	0.5777	**0.7881**	**0.5105**

Table 4: Ablation study of the proposed TransNetR on the Kvasir-SEG dataset

Method	mIoU	mDSC	Recall	Precision
TransNetR without RT block	0.7882	0.8629	0.8841	0.8923
TransNetR (RT block replaced with residual block)	0.7977	0.8669	0.8833	0.8953
TransNetR (Ours)	**0.8016**	**0.8706**	**0.8843**	**0.9073**

et al., 2021). Kvasir-SEG consisting of 1000 images, is used for training purposes. We followed the official dataset split, where 880 images are part of the training split, and the rest are reserved for testing. We performed extensive data augmentations to obtain more training samples. The cross-dataset performance is validated by evaluating the model on the other three datasets, where CVC-ClinicDB, BKAI-IGH, and PolypGen contain 612, 1000, and 1537 still images, respectively. It is worth mentioning that PolypGen incorporates data collected from six different centers covering varied populations. Thus, validation of the proposed algorithm on these types of OOD datasets makes the study more comprehensive and closer to a real-world scenario.

The proposed model is implemented using the Pytorch framework, and experiments are conducted on an NVIDIA RTX 3090 GPU system. An adam optimizer with a learning rate

Table 5: Results of the models when trained on Kvasir-SEG and tested on OOD dataset.

Method	mIoU	mDSC	Recall	Precision	F2
Training dataset: Kvasir-SEG – Test dataset: PolypGen (All)					
U-Net (Ronneberger et al., 2015)	0.5347	0.5995	0.6829	0.7523	0.6105
U-Net++ (Zhou et al., 2018)	0.5310	0.5964	0.6765	0.7546	0.6089
ResU-Net++ (Jha et al., 2019)	0.3149	0.3982	0.5887	0.4444	0.4314
HarDNet-MSEG (Huang et al., 2021)	0.5376	0.6089	0.7116	0.7124	0.6246
ColonSegNet (Jha et al., 2021)	0.4718	0.5486	0.6554	0.6687	0.5617
UACANet (Kim et al., 2021)	0.5777	0.6531	**0.7493**	0.7531	0.6678
UNeXt (Valanarasu and Patel, 2022)	0.3761	0.4552	0.6135	0.5600	0.4805
TransNetR (Ours)	**0.6058**	**0.6668**	0.7183	**0.8409**	**0.6706**
Training dataset: Kvasir-SEG – Test dataset: PolypGen (C1)					
U-Net (Ronneberger et al., 2015)	0.5772	0.6469	0.6780	0.8464	0.6484
U-Net++ (Zhou et al., 2018)	0.5857	0.6611	0.6953	0.8247	0.6700
ResU-Net++ (Jha et al., 2019)	0.4204	0.5239	0.6390	0.5789	0.5557
HarDNet-MSEG (Huang et al., 2021)	0.6256	0.7121	**0.7800**	0.7933	**0.7344**
ColonSegNet (Jha et al., 2021)	0.5514	0.6386	0.7130	0.7423	0.6551
UACANet (Kim et al., 2021)	0.6386	0.7189	0.7553	0.8476	0.7254
UNeXt (Valanarasu and Patel, 2022)	0.4481	0.5386	0.6421	0.6912	0.5686
TransNetR (Ours)	**0.6538**	**0.7204**	0.7438	**0.8778**	0.7269
Training dataset: Kvasir-SEG – Test dataset: PolypGen (C2)					
U-Net (Ronneberger et al., 2015)	0.5702	0.6338	0.7347	0.7368	0.6495
U-Net++ (Zhou et al., 2018)	0.5612	0.6240	0.7189	0.7631	0.6383
ResU-Net++ (Jha et al., 2019)	0.2779	0.3431	0.5003	0.4198	0.3606
HarDNet-MSEG (Huang et al., 2021)	0.5667	0.6311	0.7267	0.7149	0.6376
ColonSegNet (Jha et al., 2021)	0.4659	0.5371	0.6443	0.6789	0.5439
UACANet (Kim et al., 2021)	0.6091	0.6887	**0.8540**	0.6870	0.7222
UNeXt (Valanarasu and Patel, 2022)	0.3780	0.4583	0.6373	0.5239	0.4837
TransNetR (Ours)	**0.6608**	**0.7232**	0.8071	**0.8096**	**0.7366**
Training dataset: Kvasir-SEG – Test dataset: PolypGen (C3)					
U-Net (Ronneberger et al., 2015)	0.6769	0.7481	0.7637	0.8787	0.7518
U-Net++ (Zhou et al., 2018)	0.6530	0.7254	0.7526	0.8568	0.7332
ResU-Net++ (Jha et al., 2019)	0.4096	0.5109	0.6463	0.5484	0.5545
HarDNet-MSEG (Huang et al., 2021)	0.6623	0.7440	0.7947	0.8180	0.7619
ColonSegNet (Jha et al., 2021)	0.6181	0.7064	0.7520	0.7907	0.7221
UACANet (Kim et al., 2021)	0.7074	0.7870	**0.7954**	0.8893	**0.7877**
UNeXt (Valanarasu and Patel, 2022)	0.4654	0.5534	0.6265	0.6868	0.5740
TransNetR (Ours)	**0.7217**	**0.7874**	0.7904	**0.9133**	0.7863

of $1e^{-4}$ is used, and batch size is set to 8. The loss function used is a combination of binary cross-entropy and dice loss. We quantitatively compared the performance of TransNetR with SOTA methods using widely used evaluation metrics, such as mIoU, mDSC, Recall, Precision, F2, and processing speed (FPS).

3.2. Performance Evaluation

We have evaluated TransNetR performance in different scenarios. Firstly, we conducted validation tests to investigate the model's learning ability with seen data, i.e., the test split of Kvasir-SEG. This is followed by OOD testing for the generalizability test.

Learning ability: The results associated with the seen dataset are presented in Table 1. Our proposed method reported the best outcome relative to other approaches with mIoU

of 0.8016, mDSC of 0.8706, recall of 0.8843, precision of 0.9073 and F2 score of 0.8744. The performance of UACANet (Kim et al., 2021) is competitive with our method. However, TransNetR outperforms UACANet by 3.24% in mIoU and 2.04% in mDSC. Moreover, the inference time of our model is 54.60 FPS which is twice of UACANet. The qualitative results are shown in Fig. 3. It can be observed that our model has correctly segmented the polyp regions even when there is multiple polyps in the image frame and has captured relatively more accurate boundary details as compared to UACANet.

Generalization ability: We investigated the OOD outcomes that are presented in Table 2, Table 3, Table 5, and Table 6. The consistent superior performance of our model on all three still frame datasets 23 video sequence from PolypGen confirms its better generalization ability of TransNetR on different data distributions. This signifies the greater generalizing capability of TransNetR. Besides achieving a substantial difference on PolypGen (see Table 5), our proposed model outperformed the next closest competitive model, UACANet(Kim et al., 2021), by a significant margin on other polyp benchmarking datasets as well. Quantitatively, an improvement of 2.81% in PolypGen, 5.62% in PolypGen Video sequence, 1.04% in CVC-ClinicDB, and 2.64% in BKAI-IGH are reported when evaluated in terms of mIoU. Additionally, we have presented center-wise results because PolypGen images come from different centers, and each center is independent. It also helps to better analyze the models' outcomes and investigate for any biased results for specific center data. As observed from Table 5 and Table 6, all models reported similar relative differences on each center as that on the overall PolypGen dataset. Although in some cases, UACANet performed better in recall in some cases, TransNetR performed consistently superior and outperformed all the models of each center in mIoU, mDSC and precision in all cases. From the qualitative results as well, we can observe that TransNetR is better at segmentation of small, diminutive, sessile, flat and regular polyps (see Fig. 4, and Fig. 6).

Ablation study: We have presented an ablation study in Table 4 to evaluate the impact of RT block on the TransNetR model. From the results in Table 4, it can be observed that RT block boosts the performance in several performance metrics, such as 1.34% in mIoU, 0.77% in mDSC, 0.02% in recall and 1.5% in precision. As polyp segmentation is a competitive domain, even smaller improvements in the model performance can make a significant difference in clinical settings by making better disease diagnoses in terms of accuracy and efficiency.

4. Conclusion

In this work, we proposed the TransNetR, a transformer-based architecture that utilizes transformer block and residual block to segment polyps with high speed accurately. The experimental results on in-distribution and out-of-distribution data demonstrate the real-time performance of our model with promising polyp segmentation outcomes. A comprehensive comparison of our TransNet algorithm on 8 centers (6 centers from PolypGen, BKAI-IGH, and CVC-ClinicDB) datasets shows that it consistently outperforms its competitors. The qualitative and quantitative results suggest that TransNetR is more generalizable to the out-of-distribution datasets. The generalization capability of the model makes it suitable for clinical settings, and hence, TransNetR might assist clinicians in early polyp detection.

References

Mojtaba Akbari, Majid Mohrekesh, Ebrahim Nasr-Esfahani, SM Reza Soroushmehr, Nader Karimi, Shadrokh Samavi, and Kayvan Najarian. Polyp segmentation in colonoscopy images using fully convolutional network. In *Proceedings of the 2018 40th Annual International Conference of the IEEE Engineering in Medicine and Biology Society (EMBC)*, pages 69–72, 2018.

Sharib Ali, Debesh Jha, Noha Ghatwary, Stefano Realdon, Renato Cannizzaro, Osama E Salem, Dominique Lamarque, Christian Daul, Kim V Anonsen, Michael A Riegler, et al. Polypgen: A multi-center polyp detection and segmentation dataset for generalisability assessment. *Nature Scientific Data*, 2023.

Jorge Bernal, F Javier Sánchez, Gloria Fernández-Esparrach, Debora Gil, Cristina Rodríguez, and Fernando Vilariño. Wm-dova maps for accurate polyp highlighting in colonoscopy: Validation vs. saliency maps from physicians. *Computerized medical imaging and graphics*, 43:99–111, 2015.

Genta Cekodhima, Altin Cekodhima, Arben Beqiri, Mehdi Alimehmeti, and Gerhard Sulo. Demographic and histopathological characteristics of colorectal polyps: a descriptive study based on samples obtained from symptomatic patients. *Slovenian Journal of Public Health*, 55(2):118–123, 2016.

Jiawei Chen, Ziqi Zhang, Xinpeng Xie, Yuexiang Li, Tao Xu, Kai Ma, and Yefeng Zheng. Beyond mutual information: Generative adversarial network for domain adaptation using information bottleneck constraint. *IEEE Transactions on Medical Imaging*, 41(3):595–607, 2021.

Nguyen Thanh Duc, Nguyen Thi Oanh, Nguyen Thi Thuy, Tran Minh Triet, and Viet Sang Dinh. Colonformer: An efficient transformer based method for colon polyp segmentation. *IEEE Access*, 10:80575–80586, 2022.

Deng-Ping Fan, Ge-Peng Ji, Ming-Ming Cheng, and Ling Shao. Concealed object detection. *IEEE Transactions on Pattern Analysis and Machine Intelligence*, 2021.

Chien-Hsiang Huang, Hung-Yu Wu, and Youn-Long Lin. Hardnet-mseg: A simple encoder-decoder polyp segmentation neural network that achieves over 0.9 mean dice and 86 fps. *arXiv preprint arXiv:2101.07172*, 2021.

Debesh Jha, Pia H Smedsrud, Michael A Riegler, Dag Johansen, Thomas De Lange, Pål Halvorsen, and Håvard D Johansen. Resunet++: An advanced architecture for medical image segmentation. In *Proceedings of the 2019 IEEE International Symposium on Multimedia (ISM)*, pages 225–2255, 2019.

Debesh Jha, Pia H Smedsrud, Michael A Riegler, Pål Halvorsen, Thomas de Lange, Dag Johansen, and Håvard D Johansen. Kvasir-SEG: a segmented polyp dataset. In *Proceedings of the International Conference on Multimedia Modeling (MMM)*, pages 451–462, 2020.

Debesh Jha, Sharib Ali, Nikhil Kumar Tomar, Håvard D Johansen, Dag Johansen, Jens Rittscher, Michael A Riegler, and Pål Halvorsen. Real-time polyp detection, localization and segmentation in colonoscopy using deep learning. *IEEE Access*, 9:40496–40510, 2021.

Priyanka Kanth and John M Inadomi. Screening and prevention of colorectal cancer. *Bmj*, 374, 2021.

Nam Hee Kim, Yoon Suk Jung, Woo Shin Jeong, Hyo-Joon Yang, Soo-Kyung Park, Kyuyong Choi, and Dong Il Park. Miss rate of colorectal neoplastic polyps and risk factors for missed polyps in consecutive colonoscopies. *Intestinal research*, 15(3):411, 2017.

Taehun Kim, Hyemin Lee, and Daijin Kim. Uacanet: Uncertainty augmented context attention for polyp segmentation. In *Proceedings of the 29th ACM International Conference on Multimedia*, pages 2167–2175, 2021.

David A Lieberman, J Lucas Williams, Jennifer L Holub, Cynthia D Morris, Judith R Logan, Glenn M Eisen, and Patricia Carney. Race, ethnicity, and sex affect risk for polyps > 9 mm in average-risk individuals. *Gastroenterology*, 147(2):351–358, 2014.

Phan Ngoc Lan, Nguyen Sy An, Dao Viet Hang, Dao Van Long, Tran Quang Trung, Nguyen Thi Thuy, and Dinh Viet Sang. Neounet: Towards accurate colon polyp segmentation and neoplasm detection. In *Proceedings of the International Symposium on Visual Computing*, pages 15–28, 2021.

Olaf Ronneberger, Philipp Fischer, and Thomas Brox. U-net: Convolutional networks for biomedical image segmentation. In *Proceedings of International Conference on Medical image computing and computer-assisted intervention (MICCAI)*, pages 234–241, 2015.

Hyuna Sung, Jacques Ferlay, Rebecca L Siegel, Mathieu Laversanne, Isabelle Soerjomataram, Ahmedin Jemal, and Freddie Bray. Global cancer statistics 2020: Globocan estimates of incidence and mortality worldwide for 36 cancers in 185 countries. *CA: a cancer journal for clinicians*, 71(3):209–249, 2021.

Nima Tajbakhsh, Suryakanth R Gurudu, and Jianming Liang. Automated polyp detection in colonoscopy videos using shape and context information. *IEEE transactions on medical imaging*, 35(2):630–644, 2015.

Jeya Maria Jose Valanarasu and Vishal M Patel. Unext: Mlp-based rapid medical image segmentation network. In *Medical Image Computing and Computer Assisted Intervention–MICCAI 2022: 25th International Conference, Singapore, September 18–22, 2022, Proceedings, Part V*, pages 23–33. Springer, 2022.

Xiaoyong Yang, Qianxing Wei, Changhe Zhang, Kaibo Zhou, Li Kong, and Weiwei Jiang. Colon polyp detection and segmentation based on improved mrcnn. *IEEE Transactions on Instrumentation and Measurement*, 70:1–10, 2020.

Zongwei Zhou, Md Mahfuzur Rahman Siddiquee, Nima Tajbakhsh, and Jianming Liang. UNet++: a nested u-net architecture for medical image segmentation. In *Deep learning in medical image analysis and multimodal learning for clinical decision support*, pages 3–11. 2018.

Table 6: Training dataset: Kvasir-SEG – Test dataset: PolypGen (C4, C5, C6).

Method	mIoU	mDSC	Recall	Precision	F2
Training dataset: Kvasir-SEG – Test dataset: PolypGen (C4)					
U-Net (Ronneberger et al., 2015)	0.3699	0.4147	0.6550	0.5982	0.4263
U-Net++ (Zhou et al., 2018)	0.3807	0.4202	0.6337	0.6099	0.4294
ResU-Net++ (Jha et al., 2019)	0.1689	0.2268	0.6342	0.2816	0.2433
HarDNet-MSEG (Huang et al., 2021)	0.3516	0.3936	0.6758	0.5535	0.4062
ColonSegNet (Jha et al., 2021)	0.2933	0.3422	0.6493	0.4710	0.3558
UACANet (Kim et al., 2021)	0.4273	0.4828	**0.7371**	0.6301	0.4982
UNeXt (Valanarasu and Patel, 2022)	0.2261	0.2757	0.6645	0.3552	0.2989
TransNetR (Ours)	**0.4601**	**0.5042**	0.6874	**0.7141**	**0.5096**
Training dataset: Kvasir-SEG – Test dataset: PolypGen (C5)					
U-Net (Ronneberger et al., 2015)	0.2963	0.3614	0.4577	0.5497	0.3870
U-Net++ (Zhou et al., 2018)	0.3143	0.3773	0.4475	0.6030	0.3935
ResU-Net++ (Jha et al., 2019)	0.2041	0.2748	0.4643	0.3027	0.3156
HarDNet-MSEG (Huang et al., 2021)	0.3090	0.3769	0.4588	0.5250	0.3970
ColonSegNet (Jha et al., 2021)	0.2687	0.3416	0.4097	0.5232	0.3532
UACANet (Kim et al., 2021)	0.3257	0.4028	**0.4941**	0.5615	**0.4250**
UNeXt (Valanarasu and Patel, 2022)	0.2530	0.3288	0.4646	0.4192	0.3583
TransNetR (Ours)	**0.3597**	**0.4214**	0.4508	**0.7767**	0.4232
Training dataset: Kvasir-SEG – Test dataset: PolypGen (C6)					
U-Net (Ronneberger et al., 2015)	0.5384	0.6126	0.7054	0.7508	0.6362
U-Net++ (Zhou et al., 2018)	0.5355	0.6163	0.7340	0.7230	0.6564
ResU-Net++ (Jha et al., 2019)	0.2816	0.3684	0.6220	0.3526	0.4326
HarDNet-MSEG (Huang et al., 2021)	0.5548	0.6341	0.7197	0.7722	0.6487
ColonSegNet (Jha et al., 2021)	0.4410	0.5290	0.6199	0.6403	0.5424
UACANet (Kim et al., 2021)	0.6039	0.6748	**0.7698**	0.7669	**0.7028**
UNeXt (Valanarasu and Patel, 2022)	0.3743	0.4539	0.6019	0.5045	0.4850
TransNetR (Ours)	**0.6335**	**0.6917**	0.6783	**0.9431**	0.6803

Appendix Figure 6 (a) shows the example of the input image from out-of-distribution (unique medical centers (center 6 from PolypGen)), corresponding ground truth, predicted masks, and the heatmap of the intermediate feature maps of the TransNetR. The prediction results show that TransNetR is better at predicting different-sized polyps.

Figure 6 (b) shows the example of the input image from out-of-distribution (unique medical centers), corresponding ground truth, predicted masks, and the heatmap of the intermediate feature maps of the TransNetR. In the provided heatmap, the "red" and "yellow" areas represent essential features of TransNetR, and the blue area refers to the features that are not significantly important. The prediction shows that TransNetR can perform well even on small polyps, medium or regular polyps, and even with more than one polyp.

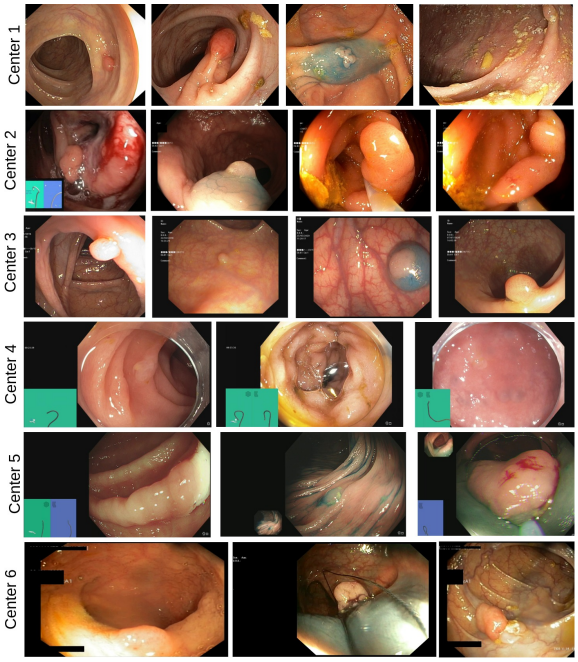

Figure 5: Center-wise example images from the PolypGen dataset. Here, the variability among the dataset from different centers can be observed. There is a difference in image resolutions and sizes, shapes, colors, textures and appearances and collection protocols.

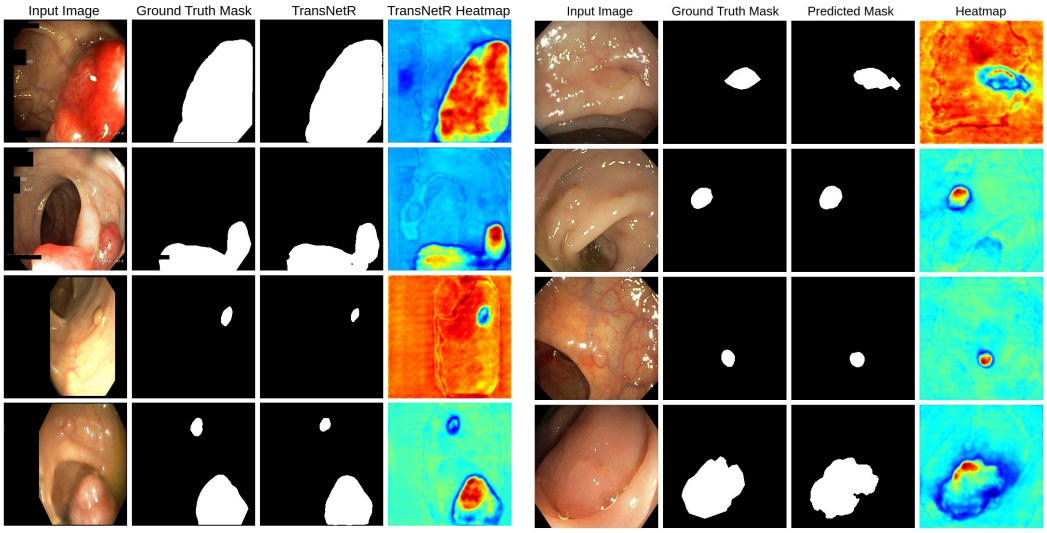

Figure 6: Qualitative result when the TransNetR is trained on Kvasir-SEG and tested on (a) PolypGen (center 6 (C6)) and (b) PolypGen (center 1 (C1)).